# MAGNETIZATION HYSTERESIS ELECTRON PARAMAGNETIC RESONANCE

## A New Null Phase Insensitive Saturation Transfer EPR Technique with High Sensitivity to Slow Motion

ARNT INGE VISTNES
*Institute of Physics, University of Oslo, Blindern, Oslo 3, Norway*

ABSTRACT In electron paramagnetic resonance (EPR) nonlinear phenomena with respect to magnetic-field modulation are often studied by out-of-phase spectra recordings. The existence of a nonzero out-of-phase signal implies that the EPR signal is phase shifted relative to the modulation signal. This phase shift is called a magnetization hysteresis. The hysteresis angle varies during a sweep through the resonance conditions for a free radical. By recording this variation, a magnetization hysteresis (MH) spectrum results. In practice, a MH spectrum is computer calculated from two EPR spectra detected with a 90° difference in phase setting. There is no need for a careful null-phase calibration like that in traditional analysis of nonlinearities. The MH spectra calculated from second harmonic EPR spectra of spin labels were highly dependent on the rotational correlation time. The technique can therefore be used to study slow molecular motion. In the present work MH spectra and Hemminga and deJager's magnitude saturation transfer EPR spectra (Hemminga, M. A., and P. A. deJager, 1981, *J. Magn. Reson.*, 43:324–327) have been analyzed to define parameters that can describe variations in the rotational correlation time. A novel modification of the sample holder and temperature regulation equipment is described.

### INTRODUCTION

Saturation transfer electron paramagnetic resonance (ST-EPR) as introduced by Thomas et al. (1976) is a very useful technique for the study of slow molecular rotational motion. The method is fairly sensitive and easy to use. However, at least two calibration problems are involved. First, it is difficult to determine the microwave magnetic field at the position of the sample and second, problems are connected with finding the correct phase setting on the phase-sensitive detector. The latter problem has been vigorously discussed. Thus, Thomas et al. (1976) introduced the "self-null" procedure, whereas Gaffney (see Hyde and Dalton, 1979) found an interpolation procedure more useful. Watanabe used a digitized ST-EPR system and Fourier transformation and evaluated the phase setting by a computer algorithm (Watanabe et al., 1980; Sasaki et al., 1980). Furthermore, Watanabe studied the influence of the estimated rotational correlation time on the phase (Watanabe et al., 1982). An accuracy of ±2 to ±3° in the phase setting yields an error of up to 30% in the correlation times. Watanabe used 100-kHz modulation (200-kHz detection), which is twice that used by most other investigators. Consequently, the data and conclusions arrived at by Watanabe et al. can only qualitatively (but not quantitatively) be applied in a normal ST-EPR experiment.

The problem with phase setting is completely avoided in the "magnitude saturation transfer EPR" (M-ST-EPR) method introduced by Hemminga and deJager (1981). They combine the in-phase $[I(B)]$ and out-of-phase $[Q(B)]$ signals for a magnetic-field setting $(B)$ and calculate the parameter $M(B)$;

$$M(B) = [I^2(B) + Q^2(B)]^{1/2}. \quad (1)$$

This parameter is calculated throughout the spectrum, and $M(B)$ is called a magnitude spectrum. Every other value of the phase setting yields the same magnitude spectrum, if the initial two phase settings are separated by 90°.

The M-ST-EPR spectrum is dominated by the in-phase signal, whose shape is less sensitive to slow motion than the ST-EPR spectrum. Consequently, the shape of the M-ST-EPR spectrum does not change very much for the rotational correlation time in the interval $10^{-7}$ to $10^{-3}$ s. The signal-to-noise ratio is, however, good, and the method is valuable in practical applications along with ST-EPR. In the present paper new parameters to study the rotational correlation time have been worked out.

The M-ST-EPR spectrum represents one way to obtain a phase-independent signal. Another possibility in which two spectra are combined to obtain a hysteresis spectrum is presented in the following. When the magnetic field is modulated in time, a magnetization hysteresis (or a phase

shift) may occur (Halbach, 1954). The magnetization hysteresis (MH) angle is given by

$$MH(B) = \text{arc tangent } [Q(B)/I(B)]. \quad (2)$$

For the moment we neglect the sign of $I$ and $Q$. The magnetization hysteresis will be zero if the modulation frequency is small compared with both $1/T_1$ and $1/T_2$ (where $T_1$ and $T_2$ are the spin-lattice and the spin-spin relaxation times for the electron). With increasing out-of-phase signal, the magnetization hysteresis will increase. Note that small out-of-phase signals influence the MH-EPR spectrum, while the M-ST-EPR spectrum remains unchanged.

Eq. 2 shows that the absolute hysteresis angle is phase dependent. However, the differences in hysteresis like

$$\Delta MH_{12} = MH(B_1) - MH(B_2) \quad (3)$$

are completely phase independent. That is, regardless of the signals used for $Q$ and $I$ in Eq. 2, any differences in the hysteresis in the spectrum will be independent of the phase setting if the $Q$ and $I$ are separated by 90°. This will be demonstrated below. The MH-EPR spectra are sensitive for several physiochemical conditions depending on whether they are calculated from first or second harmonic signals. In this work magnetization hysteresis spectra are calculated from second harmonic signals. They are rotational correlation time dependent. (MH spectra calculated from first harmonic signals can be used for microwave power calibration as discussed by Vistnes and Dalton, [1983].)

## EXPERIMENTAL

### Instrumentation

The experiments were carried out at x-band frequencies using an EPR spectrometer (ER-200D; Bruker Analytische Messtechnik, GmbH, Rheinstetten, FRG) equipped with a standard rectangular cavity. The frequency of the magnetic-field modulation was 50 kHz, and the signal was detected at 100 kHz on a ER022 modulation/receiver unit (Bruker Analytische Messtechnik, GmbH.). The modulation amplitude was 5 G as calibrated using standard procedures (Wertz and Bolton, 1972). The incident microwave power was 65 mW unless otherwise stated. This corresponds to a microwave magnetic field in the center of the sample of 0.22 G (at 60% glycerol) as determined by a combination of the perturbing sphere method (Ginzton, 1957; Freed et al., 1967) and a MH method (Vistnes and Dalton, 1983). The phase setting (null phase) was determined using Gaffney's interpolation procedure in combination with an extra amplifier (see below).

The spectra were digitized using a signal averager (PAR 4202; EG&G Princeton Applied Research, Princeton, NJ). The data were transferred to a NORD-100 minicomputer (Norsk Data A/S, Oslo, Norway) via an Apple II microcomputer (Apple Computer Inc., Cupertino, CA). The data processing was done on the NORD-100 and plotted on a 7220 A plotter (Hewlett-Packard Co., Palo Alto, CA). A built-in amplifier on the PAR averager is placed between the output from the EPR spectrometer and the analog-to-digital (A-D) converter. This amplifier was used to compensate for differences in the signal amplitudes for the two spectra ($I$ and $Q$) in a set. Thus, the 90°-detector-phase switch was the only spectrometer setting that was touched when going from an $I$ to a $Q$ recording or vice versa. Unfortunately, the PAR averager has only an 8-bit A-D converter. With this low resolution, numeric noise can be troublesome in parts of the calculated spectra. To avoid this problem, we added eight or more identical spectra, thus achieving a full-scale value of 12 bits. The corresponding result was then roughly of the same quality as if a 12 bit A-D converter were used in conjunction with single spectral recordings. We emphasize that the extra amplifier has no influence on the detection phase in contrast to the amplifier in the EPR spectrometer itself. The extra amplifier appeared to be very useful when performing the phase calibration for standard ST-EPR work. The drop in signal amplitude from 65 to 1 mW was compensated for by using this extra amplifier.

### Baseline Correction

In the current experiment either a 100 or a 200 G sweep was digitized with 1,024 point resolution. The baseline was determined by a linear interpolation between the first few and the last few points in the sweep. In the particular case of 200-G sweep, the baseline correction was accurate (as judged from the reproducibility of data). The baseline correction can be more elaborate (e.g., at poor signal-to-noise ratio). However, the baseline correction cannot be performed by the usual integration procedure when dealing with nonlinear phenomena.

### Sample Holder and Temperature Control

A new flat cell was constructed for reducing the geometrical size of the sample, which in turn implies that the microwave field and the magnetic-field modulation are fairly uniform over the sample. For example, the microwave field does not change by more than 20% based on preliminary measurements using a MH method (Vistnes and Dalton, 1983). The new flat cell was made in quartz by Hellma GmbH & Co, Müllheim-Baden, FRG. The flat part was 10-mm long, 8-mm wide, and 0.6-mm thick (inner dimensions). Tubes with 4-mm outer diameter were placed in each end of the flat portion, one with 0.6 and the other with 2-mm inner diameter. The passage between tubes and the flat portion was made by drilling a 0.6-mm hole in the end plates of the flat chamber before the tubes were fused on. Only the flat portion was filled with the sample, and the capillary end was sealed with Sigillum wax (Modulohm I/S, Herlev-Copenhagen, Denmark). Because of the small air volume between the seal and the sample, moderate temperature changes have no influence on the position of the sample.

The temperature of the flat cell was controlled using a new temperature adapter system described in Fig. 1. Cold $N_2$ gas is blown from the standard transfer Dewar into a Teflon adapter and then through a very thin walled 10-mm diameter Mylar tube. The Mylar tube was fastened between two Teflon collets at each end of the cavity. The lower collet, which was used for fastening of the flat cell, has slits in the end face to allow for the flow of cold nitrogen gas. The flat cell could also be taken out through these slits when the lower fastening nut was loosened. The upper end of the flat cell was positioned by a Teflon plunger. The flat portion of the cell was placed in the middle of the cavity by adjusting the height of the Teflon plunger. The result was controlled visually through the Perspex window in front of the irradiation slits. This height adjustment was only done once per experiment since the Teflon plunger did not alter position when the sample was changed. A flow of dry nitrogen gas at room temperature passed through the cavity. Condensation problems were completely avoided by this arrangement because the cold nitrogen gas and air met below the cavity and no cold surfaces were in contact with air.

The temperature of the cold nitrogen was controlled by the standard VT-1000 temperature controller (Bruker Analytische Messtechnik GmbH). The temperature of the sample was determined using a fluoroptic thermometer (Model 1000 A; Luxtron Corp., Mountain View, CA) equipped with an optical fiber probe (Luxtron Corp., Model GMA-2). The probe was inserted through the 2-mm inner diameter tube directly into the sample in the flat cell. Because the microwave conditions are not influenced by this probe, it could be left in position during the measurements. This arrangement made it possible to note small temperature changes in the sample (i.e., due to microwave absorption in the water).

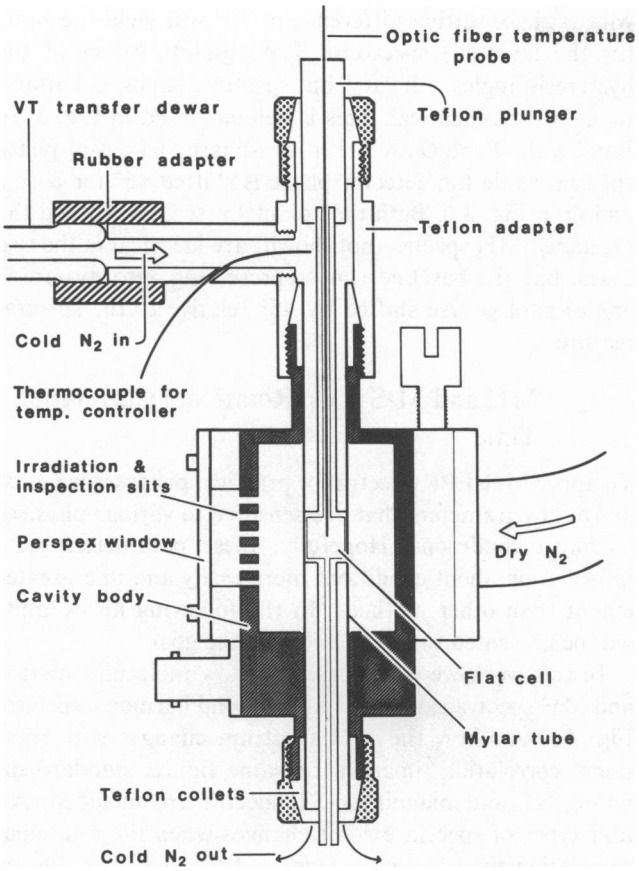


FIGURE 1 Cross section through the cavity and the temperature regulation equipment. Cold nitrogen is blown through a Teflon adapter and a Mylar tube. The temperature of the sample is monitored using an optic fiber temperature probe. The sample fills only the flat portion of the flat cell. (The flat cell is rotated 90° from its normal position for illustration.)

The model 1000 A instrument (Luxtron Corp.) available for these experiments was a first generation instrument. The long-term stability was poor and frequent calibrations were necessary. The accuracy of the temperature readings was therefore only ±2°C for some experiments in this work, especially for the lowest temperatures. (The manufacturer claims that their instruments are now greatly improved relative to the first generation instrument.) Rather large temperature gradients may occur along the Mylar tube. They are, however, less than the gradients present when the whole cavity is cooled down by blowing cold nitrogen through the irradiation slits (Thomas et al., 1976). The temperature stabilizes more rapidly when using the equipment in Fig. 1 than if the whole cavity is cooled down.

## Model System

Spin-labeled human oxyhemoglobin was used as a model for isotropic rotational motion. The isolation of the hemoglobin was carried out as described by Benesch and Benesch (1962) with a few minor modifications. The hemoglobin concentration was determined using the extinction coefficients of LaGattuta et al. (1981). The purity of the oxyhemoglobin was controlled and found to be ~ 94% using the formula of Benesch et al. (1965). The labeling of the hemoglobin was essentially done as described by McCalley et al. (1972), but the reaction temperature was ~ 20°C in ~ 30 min. The maleimide spin label (4-Maleimido-2,2,6,6-tetramethylpiperidinooxyl) was purchased from Syva Research Chemicals, Palo Alto, CA.

To obtain a slow molecular rotation, labeled hemoglobin was dissolved in a mixture of 125-mM phosphate buffer, pH 7.0, and water-free glycerol (Merck Chemical Div., Merck & Co., Inc., Rahway, NJ). The hemoglobin concentration was 2.5%. Glycerol concentrations of 40, 60, 80 and 90% (vol/vol) were used for a rough variation of the viscosity. (The volume of glycerol was determined by weight.) A finer variation was obtained by varying the sample temperature between ~ −18 and +15°C. The viscosities of the buffer-glycerol solutions (without hemoglobin) were determined using Cannon-Fenske viscosimeters (Cannon Instrument Co., State College, PA). The rotational correlation time, $\tau_c$, was then calculated using the Debye equation

$$\tau_c = 4\pi\eta R^3/(3kT). \quad (4)$$

In this formula $\eta$ is the viscosity, $R$ the radius of the hemoglobin (29 Å was used), $k$ and $T$ have their usual meanings. We have not included the increase in viscosity due to the 2.5% hemoglobin when calculating $\tau_c$. Preliminary experiments show that if this effect were included, the calculated rotational correlation times would be ~ 20% higher than the values used here.

## RESULTS

### Representation of a MH-EPR Spectrum

A representation of relative hysteresis angles as a function of the magnetic field is called here a magnetization spectrum. A MH-EPR spectrum of spin-labeled hemoglobin is given in Fig. 2. The corresponding in- and out-of-phase spectra are given at the top, while the MH spectrum is

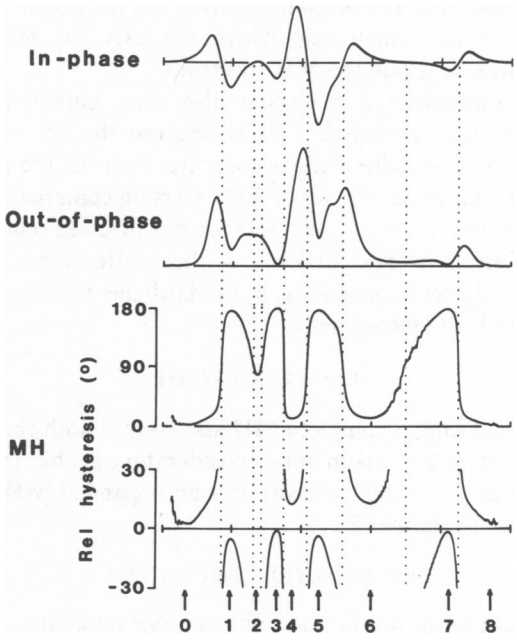


FIGURE 2 In-phase and out-of-phase second harmonic absorption spectra and the corresponding magnetization hysteresis spectra (MH). The upper MH spectrum is the complete MH representation, while the lower one is a so-called expanded representation. This is obtained in the following way. The upper half of the complete MH spectrum is subtracted by 180° while the lower half is retained. The vertical axis is expanded three times in this example and only the −30° to +30° region is given. For this reason line 2 is off scale in this particular expanded MH spectrum. The sample is spin-labeled oxyhemoglobin in 80% glycerol at 5°C, corresponding to a rotational correlation time of $8 \cdot 10^{-6}$ s. The sweep width is 100 G, the modulation amplitude 5 G, and the incident microwave power 65 mW. *Rel*, relative.

presented in two different representations at the bottom. The top MH spectrum is called a complete MH spectrum because it is continuous for all magnetic-field values. The hysteresis angle switches from 0 to 180° as the in-phase signal goes from a positive to a negative value. For a small out-of-phase signal the MH spectrum therefore looks very much like square pulses, (Fig. 4, top right). For larger out-of-phase signals, the MH spectrum becomes smoother, and the change in the hysteresis angle is smaller than 180° when the in-phase signal changes sign.

The 180° change in the hysteresis angle is due to the change in sign of the in-phase signal. If we subtract 180° from the top portions of the complete MH spectrum (for example, the parts of the MH spectrum above 150°), an expanded MH spectrum results as illustrated by the bottom MH spectrum in Fig. 2. This spectrum is discontinuous and for some magnetic-field values it is rather arbitrary whether the hysteresis angle representation should belong to the upper or lower portion of the spectrum. The vertical axis can often be expanded (blown up) without loosing details in the spectrum. Thus, small variations in the MH spectrum are more easily followed in an expanded MH spectrum compared with the complete MH spectrum. For a very small out-of-phase signal, the expanded MH spectrum is almost a straight line with eight discontinuities. The bottom spectrum of Fig. 2 is far from a straight line, which demonstrates clearly the effect of nonlinearities upon the MH spectrum.

Discontinuities may appear also when complete MH spectra are calculated. This is because the arc tangent function is periodic while a computer reduces the results within an interval of 180° or 360°. Certain combinations of $I$ and $Q$ in Eq. 2 may yield MH spectra inverted relative to those given in Fig. 2. Even if these effects are of no methodological importance, a standardizing procedure can be useful. We recommend

$$\theta' = -\arctan(I/Q) \tag{5}$$

for calculating a complete MH spectrum. (Both the signs of $I$ and $Q$ are taken into consideration.) This gives $\theta'$ values in the $\pm 180°$ interval. For an expanded MH spectrum we recommend

$$\theta = \arctan(x), \text{ where } x = Q/I. \tag{6}$$

This will result in $\theta$ in the $-90°$ to $+90°$ interval only. $I$ is the second harmonic signal, detected in the in-phase region, and $Q$ is the signal, detected in the out-of-phase region, but is 90° phase shifted relative to $I$. In this procedure, the 180° subtractions necessary for obtaining expanded MH spectra are carried out automatically.

## Phase Independence

MH spectra can be calculated using Eq. 5 or 6 with the true in-phase and out-of-phase spectra as $I$ and $Q$. However, as previously mentioned, any two signals detected with a phase setting difference of 90° will yield the same (or the inverted) spectrum. The absolute values of the hysteresis angles will vary, but spectral shapes and amplitudes will be identical. This is demonstrated in Fig. 3. In Fig. 3 *a* the $I$ and $Q$ are the true in-phase and out-of-phase spectra, while the detector phase is shifted 45° for both $I$ and $Q$ in Fig. 3 *b*. Both the complete (see figure) and the expanded MH spectra (not shown) are identical in the two cases, but the baseline (line representing zero hysteresis angle) is of course shifted by 45° relative to the spectral features.

## MH and M-ST Vs. Rotational Correlation Time

To apply MH-EPR spectra for practical purposes we must arrive at parameters that are sensitive to various physicochemical conditions. Hopefully, these parameters yield information about conditions more easily and to a greater extent than other methods. In the following an example will be presented that is in line with the goal.

In this work we concentrate on slow molecular motion and MH spectra calculated from second harmonic spectra. Fig. 4 shows how the MH spectrum changes with rotational correlation time. In the same figure, standard in-phase, ST and magnitude-ST spectra are included. All four types of spectra exhibit changes when the rotational correlation time increases from $\sim 10^{-7}$ to $10^{-4}$ s. Let us look in more detail for parameters that can describe these changes. A M-ST spectrum is complicated and contains several extrema (the points marked A–L in Fig. 5). Most of the extreme values have been analyzed for different rotational correlation times. The parameters most useful in characterizing a particular $\tau_c$ are the ratios $D/E$, $G/F$, and $I/H$. In Fig. 6 the variations of these parameters are given vs. the correlation time. A detailed study of the spectral

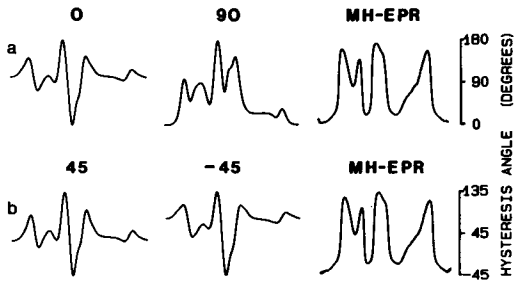


FIGURE 3 The influence of the detection-phase setting on the MH-EPR spectrum. In the upper part the in-phase and the out-of-phase spectra are used for calculating the MH signal. Underneath the detection-phase setting is shifted ~45° relative to the upper spectra. For the corresponding MH spectra, the calculated hysteresis angles are shifted 45° relative to each other. The shape and amplitude of the MH spectra, however, are identical in the two cases. Similar results are obtained for any two spectra that are recorded with a detection-phase setting difference of 90°. All the second harmonic spectra are scaled to the same maximum amplitude. In calculating a MH spectrum the relative amplitudes, e.g., between an in-phase and an out-of-phase spectrum, have to be taken into account.

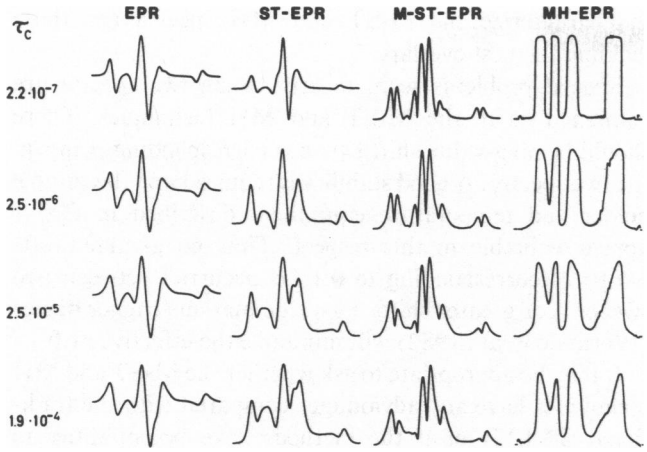


FIGURE 4 The conventional in-phase EPR spectrum, the saturation transfer (ST), the magnitude saturation transfer (M-ST), and the magnetization hysteresis (MH) EPR spectra for various rotational correlation times ($\tau_c$). The MH signals represent the complete MH spectra (see text). The ratios between the maximum amplitudes (*top to bottom*) for the in-phase and the ST-ESR signals are: 11.8, 8.1, 6.0, and 3.7. The glycerol concentration (in percent) and the sample temperatures were 40, 60, 80, and 90%, and 9°, −7°, −6°, and −10°C, respectively (*top to bottom*); otherwise as for Fig. 2.

characteristics reveals that certain amplitudes (like *C*, *F*, and *H*) are dominated by the in-phase signal while others (like *B*, *G*, and *I*) are dominated by the out-of-phase signal. Note that two of the parameters just mentioned ($G/F$ and $I/H$) represent the ratio between an out-of-phase signal and a nearby in-phase signal and are therefore related to the hysteresis angle.

The magnetization hysteresis representation is simpler

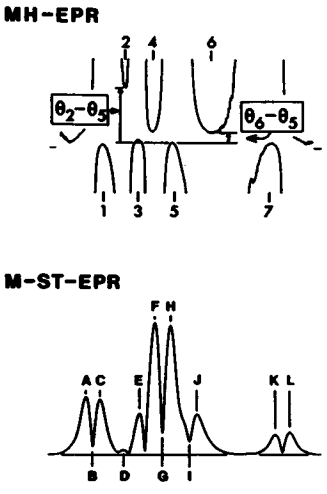


FIGURE 5 *Upper*, the expanded MH spectrum including a numbering of the intervals as well as a definition of parameters used to characterize the signal. Note that the ordinate in a MH spectrum has the unit degree. The amplitude is therefore completely independent of the spin-label concentration. *Lower*, the M-ST spectrum with lettering of positions that yield extreme values. The letter is used as a measure of the amplitude in that particular position. The amplitude increases in proportion to the spin-label concentration.

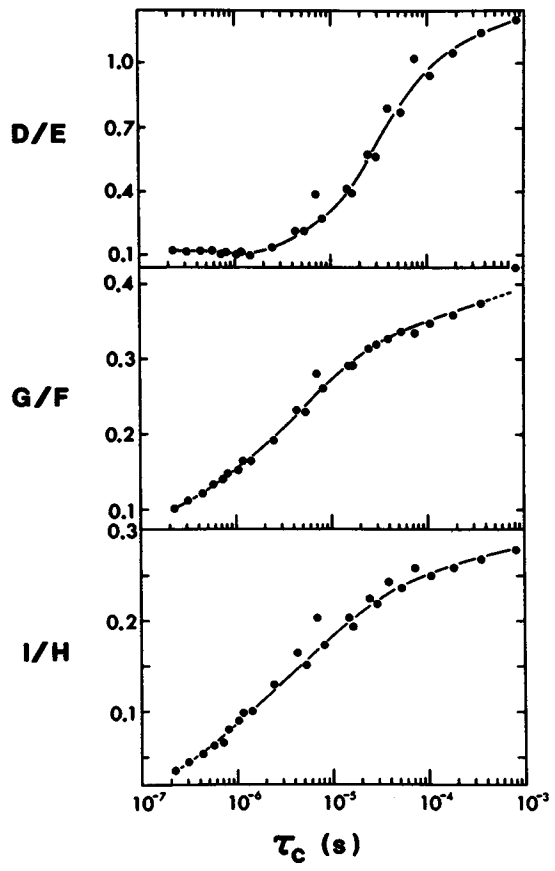


FIGURE 6 Variation of three M-ST parameters with rotational correlation time.

than the M-ST spectrum. If the expanded MH spectrum is divided into 9 intervals (as indicated in Fig. 2), only one extreme value is obtained in the intervals 1 to 7. The variation of the hysteresis angle ($\theta_1$ to $\theta_7$) with the rotational correlation time has been followed for these regions. Three parameters that appear very sensitive to spectral changes are $\theta_2-\theta_5$, $\theta_3-\theta_5$, and $\theta_6-\theta_5$. Fig. 5 illustrates how these parameters can be determined from an expanded MH spectrum. The variation of these parameters with the rotational correlation time is given in Fig. 7. The unit for a hysteresis angle difference is degrees.

The $\theta_5$ angle is more accurately determined than any of the other hysteresis angles. Therefore $\theta_5$ is used as a common reference for all three parameters in Fig. 7. The parameter $\theta_4-\theta_5$ gave nearly identical results to $\theta_6-\theta_5$ throughout the $\tau_c$ interval tested. This parameter can also be used, but as discussed below this parameter is more microwave power dependent than $\theta_6-\theta_5$.

## DISCUSSION

Three different parameters, easily obtainable from an expanded MH-EPR spectrum, have been defined and used to study rotational correlation times in the interval $10^{-7}$ to $10^{-3}$ s (Fig. 7). The $\theta_2-\theta_5$ parameter increases by ~ 80° for

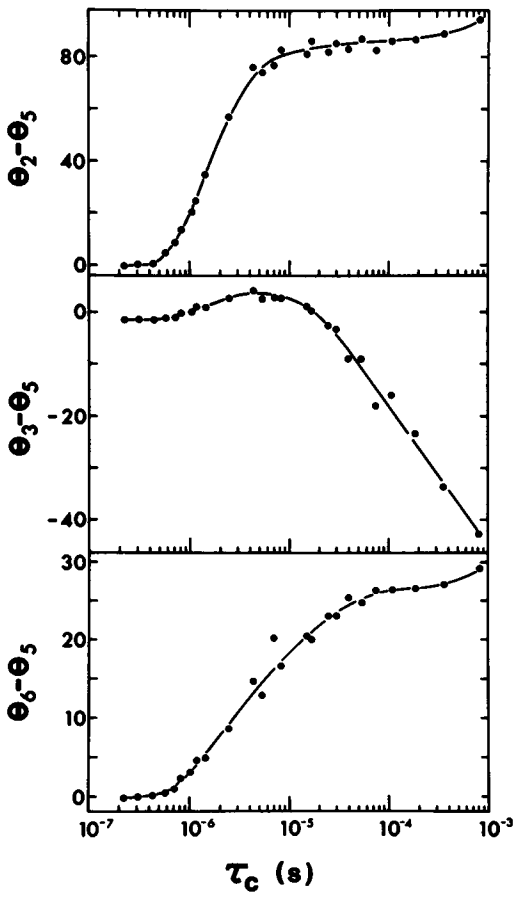


FIGURE 7 Variation of three MH parameters with rotational correlation time. The unit of the ordinate is degree.

a change of one order of magnitude in $\tau_c$. This is a very large change that demonstrates the usefulness of this parameter in discriminating small variations in $\tau_c$ (if $\tau_c$ is in the interval $10^{-6}$ to $10^{-5}$ s). The parameter $\theta_3 - \theta_5$ is sensitive in the $\tau_c$ region from $10^{-5}$ to $10^{-3}$ s where it changes by ~ 40°. The shape of the middle curve in Fig. 7 seems to suggest that this parameter is suited to study very slow motion, and thus extend the $\tau_c$ region attainable.

Figs. 6 and 7 show that the experimental points are somewhat scattered relative to the solid drawn line. Because repeated measurements at one particular glycerol concentration and $\tau_c$ value yield good reproducability (of the size of the dots in the figures), this scattering seems to be due to some systematic error. It appears that experimental data from one glycerol solution do not always overlap completely with data from another solution (with a different glycerol concentration), even if the calculated rotational correlation time is the same. Several reasons can be suggested for this apparent discrepancy. Thus, Ohnishi and co-workers (Kusumi et al., 1980) found that the microwave power varied significantly with the glycerol concentration and also with the temperature (for a constant glycerol concentration). We have made no attempts to correct for this effect. However, the parameters chosen to characterize the M-ST and MH spectra are those yielding the best overlap.

Special problems seem to arise when two spectra are combined as in the M-ST and MH techniques. There should be no g-value shift between corresponding points in the two spectra. A good stability is required and the sample holder and temperature equipment described in Fig. 1 appear valuable in this respect. Thus no g-value shifts $>6.10^{-5}$ (corresponding to 0.1 G) occurred between two sweeps. For greater shifts a g-value marker/trigger device (Wormald et al., 1982) will minimize the effective drift.

It may be appropriate to ask whether the M-ST and MH techniques have any advantages compared with the traditional ST-EPR or if the methods have potentialities to explore regions (in particular slower motion) not available with other methods. The possibilities seem to exist, but only experiments can give the answer. M-ST and MH techniques have one limitation because a computer is required for practical purposes. If this computer is reasonably fast, the time consumption for obtaining MH or M-ST spectra is equal to that for a ST spectrum. The reason is that an accurate phase calibration must be carried out for each ST spectrum while this procedure is completely eliminated for M-ST and MH work. The MH spectra may be sensitive to anisotropic motion in a way different from that for traditional ST spectra. Further studies are required to explore the potentials of the MH-method. The method seems valuable for nonlinear phenomena where the out-of-phase signals are small as shown by Vistnes and Kravdal (manuscript in preparation).

## REFERENCES


Benesch, R. E., and R. Benesch. 1962. The influence of oxygenation on the reactivity of the -SH groups of hemoglobin. *Biochemistry.* 1:735–738.

Benesch, R., G. MacDuff, and R. E. Benesch. 1965. Determination of oxygen equilibria with a versatile new tonometer. *Anal. Biochem.* 11:81–87.

Freed, J. H., D. S. Leniart, and J. S. Hyde. 1967. Theory of saturation and double resonance effects in ESR spectra. III. rf coherence and the line shapes. *J. Chem. Phys.* 47:2762–2773.

Ginzton, E. L. 1957. Microwave Measurements. McGraw-Hill Inc., New York. 515.

Halbach, K. 1954. Über eine neue Methode zur Messung von Relaxationzeiten und über den Spin von Cr.[53] *Helv. Phys. Acta.* 27:259–282.

Hemminga, M. A., and P. A. deJager. 1981. Magnitude saturation transfer electron paramagnetic resonance spectroscopy: A new ST-EPR technique insensitive to the null-phase setting. *J. Magn. Reson.* 43:324–327.

Hyde, J. S., and L. R. Dalton. 1979. Saturation transfer spectroscopy. In Spin Labeling II. L. J. Berliner, editor. Academic Press Inc., New York. 1–70.

Kusumi, A., T. Sakaki, T. Yoshizawa, and S. Ohnishi. 1980. Protein-lipid interaction in rhodopsin recombinant membranes as studied by protein rotational mobility and lipid alkyl chain flexibility measurements. *J. Biochem. (Tokyo).* 88:1103–1111.

LaGattuta, K. J., V. S. Sharma, D. F. Nicoli, and B. K. Kothari. 1981. Diffusion coefficients of hemoglobin by intensity fluctuation spectroscopy. Effects of varying pH and ionic strength. *Biophys. J.* 33:63–80.

McCalley, R. C., E. J. Shimshick, and H. M. McConnell. 1972. The effect of slow rotational motion on paramagnetic resonance spectra. *Chem. Phys. Lett.* 13:115–119.

Sasaki, T., Y. Kanaoka, T. Watanabe, and S. Fujiwara. 1980. A digitized EPR system and its application to saturation transfer electron paramagnetic resonance spectroscopy. *J. Magn. Reson.* 38:385–390.

Thomas, D. D., L. R. Dalton, and J. S. Hyde. 1976. Rotational diffusion studied by passage saturation transfer electron paramagnetic resonance. *J. Chem. Phys.* 65:3006–3024.

Vistnes, A. I., and L. R. Dalton. 1983. Experimental methods to determine the microwave field strength in electron spin resonance. *J. Magn. Reson.* In press.

Watanabe, T., T. Sasaki, K. Sawatari, and S. Fujiwara. 1980. A new detection system of saturation transfer electron paramagnetic resonance spectroscopy by a Fourier transformation technique. *Appl. Spectrosc.* 34:456–460.

Watanabe, T., T. Sasaki, and S. Fujiwara. 1982. Phase dependence of saturation transfer EPR signals and estimated rotational correlation times. *Appl. Spectrosc.* 36:174–178.

Wertz, J. E., and J. R. Bolton. 1972. Electron Spin Resonance, Elementary Theory and Practical Applications. McGraw-Hill Inc., New York. 497.

Wormald, D. I., E. Sagstuen, and A. I. Vistnes. 1982. Microprocessor-based unit for measurement of spectroscopic splitting factors (g-factors) in electron paramagnetic resonance spectroscopy. *Rev. Sci. Instrum.* 53:60–66.